European Cells and Materials Vol.54 2025 (pages 1–15) DOI: 10.22203/eCM.v054a01 ISSN 1473-2262

Original Article

COMPARISON OF HUMAN JUVENILE AND ADULT DONOR-DERIVED CHONDROCYTE SHEETS FOR SCALABLE ALLOGENEIC REGENERATIVE THERAPY

M. Kondo[1,*], K. Matsukura[1], A.J. Ford[1], N.F. Metzler[1,2], T.G. Maak[3], D.T. Hutchinson[3,4], A.A. Wang[3,4], M. Sato[5], D.W. Grainger[1,2] and T. Okano[1,6,*]

[1]Cell Sheet Tissue Engineering Center (CSTEC), Department of Molecular Pharmaceutics, Health Sciences, University of Utah, Salt Lake City, UT 84112, USA
[2]Department of Biomedical Engineering, University of Utah, Salt Lake City, UT 84112, USA
[3]Department of Orthopaedics, School of Medicine, University of Utah, Salt Lake City, UT 84108, USA
[4]Pediatric Orthopaedic Surgery, Intermountain Primary Children's Hospital, Salt Lake City, UT 84113, USA
[5]Department of Orthopaedic Surgery, Surgical Science, Tokai University School of Medicine, 259-1193 Isehara, Japan
[6]Institute of Advanced Biomedical Engineering and Science, Tokyo Women's Medical University, 162-8666 Tokyo, Japan

Abstract

Background: Regeneration of damaged cartilage is challenging, and no reproducible regenerative therapies using mass-producible cell products have been established. This study evaluated the cartilage regeneration capability and therapeutic scalability using cell sheets derived from routinely available surgical waste cartilage tissues of young and adult patients, while also investigating the mechanisms that define the characteristics of each cell type. **Methods:** We compared the viability, proliferation, and cell sheet characteristics of juvenile cartilage-derived chondrocytes (JCCs) from patients with polydactyly (2.2 ± 1.6 years) and adult cartilage-derived chondrocytes (ACCs) from patients with femoroacetabular impingement (FAI) (34.1 ± 10.6 years) *in vitro*. The *in vivo* cartilage regeneration capability of each cell sheet was validated in a nude rat knee cartilage defect model using histological O'Driscoll score evaluation on Safranin-O-stained tissues and immunohistochemistry. JCC sheets (n = 13) and ACC sheets (n = 8) were analyzed using established bulk RNA sequencing pipelines for gene ontology (GO) analysis, gene set enrichment analysis (GSEA), and ingenuity pathway analysis (IPA). Interferon gamma (IFN-γ) was applied to JCC sheet culture for confirmation of the interferon signaling involvement in cell proliferation, cell sheet characteristics, and chondrogenic differentiation. **Results:** JCC demonstrated higher colony-forming ability and stable high proliferation compared to ACC. Both JCC and ACC sheets formed positively stained hyaline cartilage for Safranin-O, type II collagen, aggrecan, and human vimentin, while being negative for type I collagen, four weeks after rat transplantation. However, the regenerated cartilage from ACC sheet transplantation was found to be thinner compared to that from JCC sheet transplantation. Comprehensive gene analysis revealed significant activation of IFN signaling in the ACC sheets. Furthermore, the addition of exogenous IFN dramatically reduced the proliferation and cartilage formation capability of JCC. **Conclusions:** JCC sheets exhibit high therapeutic scalability due to their proliferation and cartilage regeneration capabilities presumably derived from sustained low IFN-γ activity. Consideration of the donor age and tissue inflammatory status is essential for the cell source in allogeneic cell therapies. Given their sustainable sourcing from routine surgical discards, JCCs present a commercially viable and scalable option for allogeneic regenerative therapy in cartilage repair.

Keywords: Tissue engineering, cartilage regeneration, juvenile cartilage-derived chondrocytes, global gene expression, interferon signaling.

***Address for correspondence**: M. Kondo, Cell Sheet Tissue Engineering Center (CSTEC), Department of Molecular Pharmaceutics, Health Sciences, University of Utah, Salt Lake City, UT 84112, USA. Email: makoto.kondo@utah.edu; m-kondo@g.ecc.u-tokyo.ac.jp; T. Okano, Cell Sheet Tissue Engineering Center (CSTEC), Department of Molecular Pharmaceutics, Health Sciences, University of Utah, Salt Lake City, UT 84112, USA; Institute of Advanced Biomedical Engineering and Science, Tokyo Women's Medical University, 162-8666 Tokyo, Japan. Email: teruo.okano@utah.edu.

Introduction

Improved methods of cartilage repair are required to address increasing patient needs complicated by the recognized lack of innate cartilage regenerative capacity [1]. Focal cartilage defects represent a growing and known risk factor for early osteoarthritis [2,3]. Pain management does not reverse cartilage tissue degeneration. Auto- and allo- graft cartilage tissues have both been used clinically, but limited graft tissue availability and donor tissue congruity to the defect shape are unsolved issues [4,5]. Several regenerative cell therapies using autologous cells, such as chondrocytes and mesenchymal stromal cells, and recently genetically modified pluripotent cells, are currently in clinical trials [6–9]. Allogeneic cell sources are attractive for commercially feasible off-the-shelf cell therapy; regenerative therapies using reliable, mass-producible cell products are being investigated. Among them, juvenile cartilage-derived chondrocytes represent a promising cartilage-derived cell source that exhibit high proliferative and differentiation capacities [10–12]. Interestingly, juvenile cartilage-derived chondrocytes are also reported to exhibit immune-evasive properties [13].

Commercial poly(*N*-isopropylacrylamide)-grafted temperature-responsive cell culture surfaces facilitate fabrication and scaling of scaffold-free cell sheets of confluently cultured cells [14–16]. Cell sheets retain their endogenous extracellular matrix, facilitating transplant to target tissue and organ sites with high efficiency, cell survival and retention. Sheets of various cell types have been autologously and allogenically applied to multiple clinical indications in patients [17–22].

In cartilage repair, a small clinical cohort study utilized autologous adult chondrocyte sheet transplantation with concomitant reconstructive surgery to demonstrate safety and clinical efficacy in regenerating hyaline cartilage [23]. Further, polydactyly-derived chondrocyte sheets were compared to adult chondrocyte sheets fabricated from adult tissue discards obtained from patients undergoing total knee arthroplasty (TKA), showing practical advantages useful to future cartilage repair [24]. Safety and cartilage regenerative efficacy of human juvenile chondrocyte sheets were recently demonstrated in a rodent focal chondral defect model [25] and further in a small cohort of human osteoarthritis patients [26]. Despite these interesting results, direct comparisons of *in vivo* cartilage regenerative efficacy for chondrocyte sheets derived from relatively young adult and juvenile sources using identical sheet production methods have not been reported.

The current study addresses this knowledge gap by comparing the cartilage regenerative potential and the scalability of cell sheet production for two commonly available sources of cartilage tissue that have been discarded from surgical procedures: (1) juvenile cartilage-derived chondrocytes (JCCs) sourced from polydactyly removal surgeries and (2) adult cartilage-derived chondrocytes (ACCs) sourced from the femoral head during femoroacetabular impingement (FAI) repair surgeries. Cell sheet generated from both JCCs and ACCs were evaluated *in vitro* and *in vivo* using an established rat focal osteochondral defect model [25]. Differentially activated signaling responses for JCC versus ACC sheet cultures are described and attributed to characteristics distinguishing scalable sheet production based on cell growth, passaging, sheet properties and rodent defect model regenerative efficacy. Assessment of such cell sheet scalability comparisons will help validate further development of efficacious cell-based therapeutics with potential commercial viability in cartilage repair.

Materials and Methods

Cartilage Collection from Juvenile and Adult Human Polydactyly Donors

Juvenile cartilage samples were obtained from the phalanx and metacarpal bones of amputated polydactylous digits (fingers and toes) from 16 patients aged 2.2 ± 1.6 years. These tissues were sharply excised with a scalpel and immediately placed in saline after extraction. All participants were prospectively enrolled at Intermountain Primary Children's Hospital (Salt Lake City, UT, USA). For adult donors, chondrocytes were extracted from non-traumatized regions of the femoral heads of 14 patients diagnosed with femoroacetabular impingement (average age 34.1 ± 10.6 years). Specific protocols for FAI tissue harvesting are detailed elsewhere [27], and the cell isolation technique applied was consistent with that used for juvenile cartilage samples.

Chondrocyte Isolation

Following previously established protocols [25,27], fresh cartilage tissues from both juvenile and FAI donors were immersed in saline, finely cut into fragments smaller than 1 mm^2 (surface area; collected tissues were flat, so dimensions are expressed in mm^2 rather than volume) using a scalpel, and digested with 5 mg/mL type I collagenase (LS004197, Worthington Biochemical, Lakewood, NJ, USA) at 37 °C for 1.5 to 3.0 hours. The resulting cell suspensions were filtered using a 100-μm strainer, rinsed with saline, and subsequently suspended in chondrocyte isolation medium (Dulbecco's Modified Eagle Medium/Nutrient Mixture F-12 (DMEM-F12), 11320082, ThermoFisher, Waltham, MA, USA), supplemented with 1 % antibiotic-antimycotic (15240062, ThermoFisher) and 20 % fetal bovine serum (FBS) (16000044, ThermoFisher).

Cell Culture

Chondrocytes isolated from juvenile polydactyly donors (JCCs) and adult femoroacetabular impingement donors (ACCs) were seeded onto polystyrene culture dishes (229620, CELLTREAT, Pepperell, MA, USA) at a density of 5000–10,000 cells/cm^2 in chondrocyte isolation medium as previously described [25]. On day 4, during the

first media change, this medium was replaced with chondrocyte culture medium supplemented with 100 μg/mL of L-ascorbic acid phosphate magnesium salt n-hydrate (013-12061, Fujifilm Wako Pure Chemical, Osaka, Japan). Cells were subsequently passaged using this supplemented medium throughout culture. Sub-confluent cells were harvested using TrypLE Select (12563011, ThermoFisher), and cell counts were recorded. Expanded cells were cryopreserved at the end of primary passage (P0) using STEMCELLBANKER good manufacturing practice (GMP) grade solution (11924, Zenoaq, Fukushima, Japan). Thawed cells were seeded at an initial density of 10,000 cells/cm^2 and subcultured every 3–5 days using the ascorbate-containing chondrocyte culture medium.

Mycoplasma contamination, analysis performed by third-party fee-for-service, was not detected in any of the six primary cell lines (three JCC lines and three ACC lines). The identity of these donor-derived chondrocytes was confirmed by short tandem repeat (STR) profiling performed by third-party fee-for-service, showing that all lines were unique according to the STR database of the Deutsche Sammlung von Mikroorganismen und Zellkulturen (DSMZ).

Chondrocyte Sheet Preparation

Both JCC and ACC sheets were prepared according to previous JCC studies [24,25]. Briefly, cell sheets from both juvenile JCC and adult ACC cells were prepared from thawed passage 1 (P1) cells. Sub-confluent P1 cells were collected with 1x TrypLE Select for 5 minutes, then seeded at a density of 10,000 cells/cm^2 on thermo-responsive cell culture inserts (4.2 cm^2) (CS3008, CellSeed, Tokyo, Japan). Cells were cultured in ascorbic acid-containing chondrocyte culture media with medium change every 2–4 days. After 2 weeks of culture, cell sheets formed spontaneously and were harvested with forceps after room temperature incubation as contiguous, robust single constructs. Supporting ring membranes were placed over cell sheets to measure original cell sheet thickness before sheet contraction.

Cell Viability and Quantification of Chondrocyte Sheets

To prepare single-cell suspensions from adherent chondrocyte sheets, cells were first incubated with TrypLE Select for 10–15 minutes, followed by treatment with 0.25 mg/mL collagenase P (11 213 857 001, Roche, Basel, Switzerland) for 30–45 minutes. Cell counts were performed using a hemocytometer, and viability was assessed via exclusion of trypan blue dye (T8154, MilliporeSigma, Burlington, MA, USA).

Colony Forming Assay

Colony forming assay was performed by modifying previous reports [28–30]. One hundred primary isolated chondrocytes were seeded into 100-mm diameter dishes with chondrocyte isolation medium, then changed with ascorbic acid-containing chondrocyte culture medium at day 4, then replaced twice and maintained in culture for 16 days. Colonies were stained with crystal violet (C0775, Sigma-Aldrich, St. Louis, MO, USA) and >50-cell clusters were counted as a colony. Colony forming efficiency was calculated as (counted number/seeded number × 100 (%)).

Surgical Procedures for Cartilage Defect Creation and Chondrocyte Sheet Implantation

Rat surgeries and implantation of human-derived chondrocyte sheets were performed as previously described [25]. All animals were sacrificed using CO_2 after a 4-week study period.

Nude rats (RNU strain, 6–7 weeks old, both sexes; Charles River Laboratories, Wilmington, MA, USA) were acclimated in the animal facility for one week prior to surgery. Anesthesia was administered using isoflurane in combination with oxygen gas. A medial parapatellar incision was made on the right knee to expose the joint; the patella was dislocated laterally, and a focal osteochondral defect (2 mm diameter; 200–350 μm depth) was created on the femoral patellar groove using an electric grinder, ensuring no penetration into the bone marrow. The defect size and depth were precisely controlled under a surgical stereo zoom microscope (SZX10, Olympus, Tokyo, Japan).

JCC and ACC sheets prepared using temperature-responsive cell culture inserts (described above) were washed with saline, allowed to spontaneously contract to flat sheets, then cut into halves with a razor. Single sheet halves were transplanted to completely cover each surgical knee defect after defect creation. Cell sheets were held within each defect for 30–60 minutes under patella placement without suturing. Then each treated site was closed with overlying muscle suturing and skin staples. All animals received buprenorphine for 2 days and carprofen for 3 days in compliance with Institutional Animal Care and Use Committee (IACUC) protocols. Animals were sacrificed by CO_2 after 4 weeks, and knee joints harvested for further histological evaluations per previously reported protocols [25]. Experimental conditions and sample size: single ACC sheet treatment (n = 5), bilayer ACC sheet treatment (n = 6), single JCC sheet treatment (n = 6), defect only (n = 4). Animal numbers were determined using an alpha value of 5 % and 80 % power using pilot study results. Human cell sheets from 3 ACC donors and 2 JCC donors were randomly allocated for transplantation. All animals used were employed for analysis with no exclusion.

Histological Analysis

Harvested chondrocyte sheets were fixed in 4 % paraformaldehyde for 30 minutes. Rat knee joint tissues from defect models were similarly fixed in 4 % paraformaldehyde for four days, followed by decalcification using RapidCal Immuno (6089, BBC Biochemical, Mount Vernon, WA, USA) for one day. Specimens were

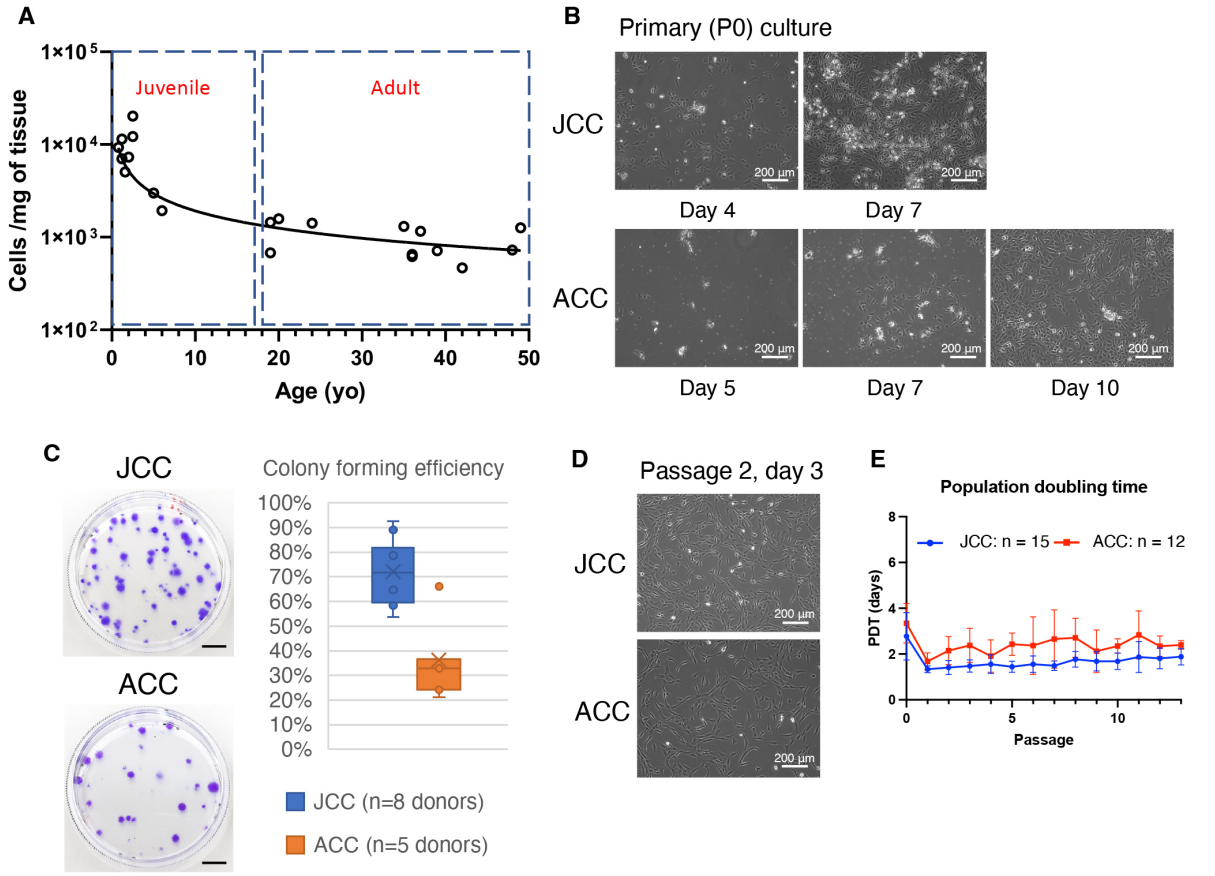

Fig. 1. Comparing culture scalability of juvenile and adult surgical discard-derived chondrocytes. (**A**) Available cell number per tissue mass as a donor cell source. Graph was prepared using GraphPad Prism. (**B**) *In vitro* expansion of juvenile (JCC) and adult (ACC) cartilage-derived chondrocytes. Juvenile cartilage-derived chondrocytes show rapid cell proliferation in primary culture. Scale bars: 200 μm. (**C**) Representative colony forming assay plate and quantification of colony forming efficiency (JCC: n = 8; ACC: n = 5 individual donors). Bars: 1 cm. Graph was prepared with Microsoft Excel. (**D**) Phase contrast images of passage cultured chondrocytes. Scale bars: 200 μm. (**E**) Population doubling time (PDT) of JCCs and ACCs. Data shown as mean and SD (JCC (blue): n = 15; ACC (red): n = 12 individual donors).

embedded in paraffin blocks and sectioned transversely at 5 μm thickness using a microtome. Sections were deparaffinized by baking at 65 °C and sequential washes with xylene and ethanol, then rehydrated via gradual ethanol replacement with distilled water.

Safranin-O staining was performed to visualize sulfated glycosaminoglycans. Samples were first treated with Weigert's Iron Hematoxylin (115973, MilliporeSigma) for five minutes, followed by five minutes in 0.5 g/L Fast Green FCF (F7258, MilliporeSigma), and finally five minutes in 0.1 % Safranin-O (TMS-009, MilliporeSigma). Microscopic imaging was conducted using a BX41 microscope (Olympus, Tokyo, Japan), and images were processed using AmScope software (v.10.11.2024, Irvine, CA, USA).

Histological evaluation of knee samples was conducted by following previous reports employing modified O'Driscoll scoring system regarding (I) nature of predominant tissue, (II) structural characteristics, (III) freedom from cellular changes of degeneration, (IV) freedom from degenerative changes in adjacent cartilage, (V) subchondral bone, and (VI) Safranin-O staining [31,32]. Safranin-O-stained samples of rat knee samples were allocated to histological assessment by multiple evaluators. Evaluators blindly tested the histological samples. Neocartilage thickness was measured by averaging 3 vertical lines across each defect section, then average thickness and standard deviation was calculated from n = 4–6 different knee samples.

Immunohistochemistry

Histological sections were rehydrated for antigen retrieval, using a method optimized to maintain tissue integrity in both rat knee and cell sheet samples. Protease

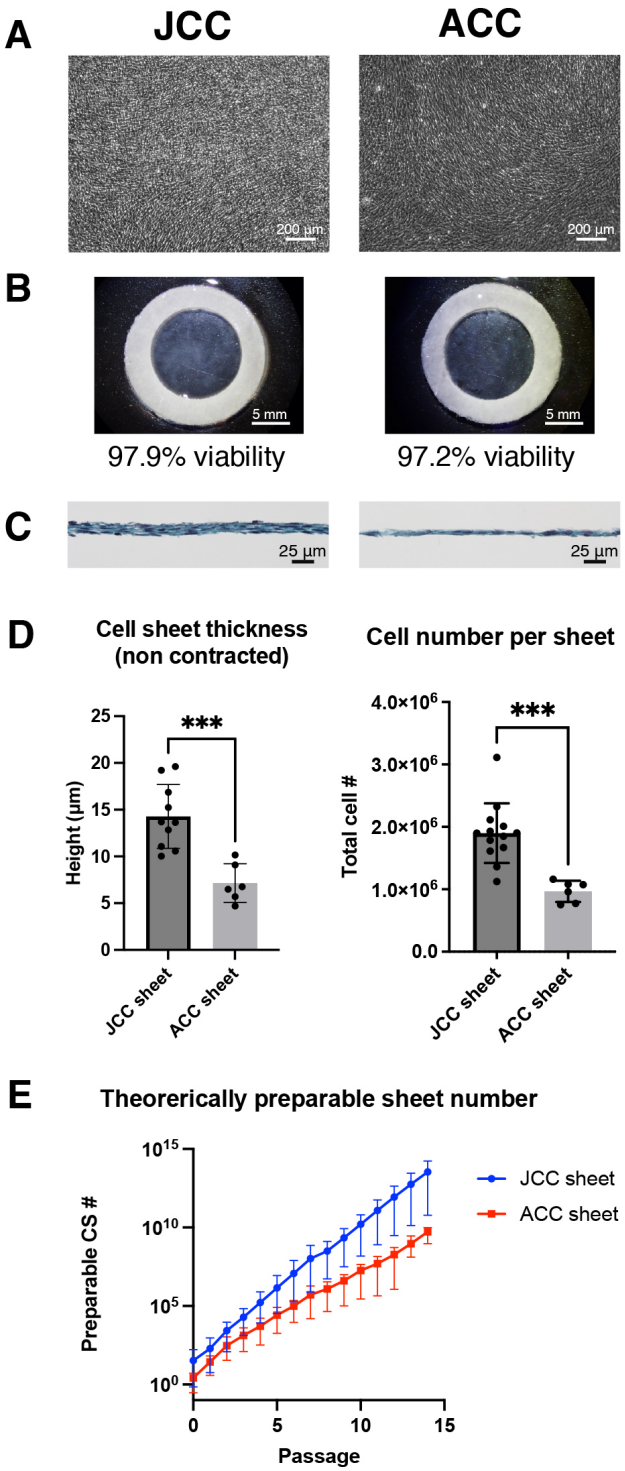

Fig. 2. Comparisons of fabricated JCC and ACC sheets. (**A**) Phase contrast image of confluent JCCs (left) and ACCs (right) from passage 2 at day 14 ready for cell sheet harvest by temperature reduction. Scale bar: 200 μm. (**B**) Macroscopic images of the harvested sheet with supporting ring membrane. Scale bar: 5 mm. (**C**) Safranin-O staining examples of JCC and ACC sheets. Bars: 25 μm. (**D**) Cell sheet thickness and total cell number in one cell sheet. Plots represent individual donor-derived cell sheets. ***$p < 0.001$ by unpaired *t*-test (left) and Mann-Whitney test (right). (**E**) Comparison of theoretical numbers of ACC versus JCC cell sheets produced from routine passage cultures. Numbers for passage 2 are shown as a current JCC clinical translational protocol setting. Data shown as mean and SD (JCC: n = 14; ACC: n = 11 individual donors). Graphs of **D** and **E** were prepared using GraphPad Prism.

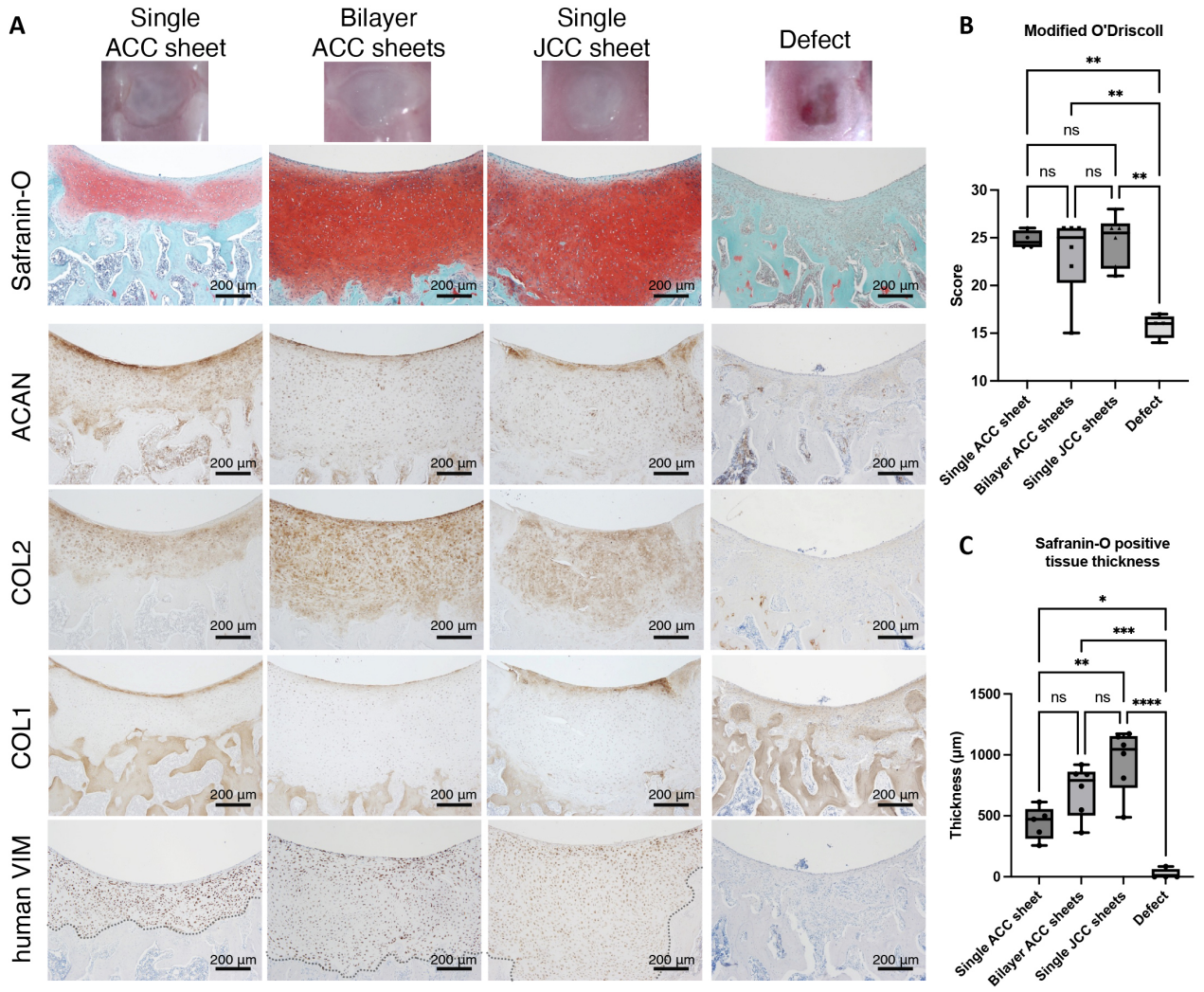

Fig. 3. Comparison of *in vivo* JCC versus ACC cell sheet efficacy in nude rat focal chondral defect treatments. (**A**) Macroscopic images of surgically created focal defects and Safranin-O, aggrecan (ACAN), type II collagen (COL2), type I collagen (COL1), and human vimentin (VIM) staining at 4 weeks after cell sheet treatments. Bars: 200 μm. Dotted lines denote donor and host tissue interfaces with no gaps. (**B**) Modified O'Driscoll scores for each condition. Data are shown as min. to max. whisker with data plots of individual animals after averaging quantified values. $^{**}p < 0.01$ with analysis of variance (ANOVA) and Tukey test. (**C**) Regenerated cartilage thickness of each condition at 4 weeks. Data are shown as min. to max. whisker with data plots of individual animals after averaging quantified values. *, **, ***, and $^{****}p < 0.05$, 0.01, 0.001, and 0.0001, respectively with ANOVA and Tukey test. Graphs **B** and **C** were prepared using GraphPad Prism.

K (S3020, Agilent Technologies, Santa Clara, CA, USA) was selected for retrieval to enhance staining for type II collagen (COL2) and human vimentin (hVIM) in knee tissue. Endogenous peroxidase activity was blocked with hydrogen peroxide (216763, MilliporeSigma). Blocking was then carried out with 5 % donkey serum and 0.1 % Triton-X in phosphate-buffered saline (PBS) for one hour at room temperature.

Following blocking, tissue sections were incubated overnight at 4 °C with primary antibodies. These included polyclonal goat anti-type I collagen (COL1) (1:200, 1310-01, SouthernBiotech, Birmingham, AL, USA), monoclonal mouse anti-type II collagen (COL2) (1:200, 2B1.5, ThermoFisher), polyclonal goat anti-aggrecan (ACAN) (1:100, AF1220, R&D Systems, Minneapolis, MN, USA), and monoclonal rabbit anti-human vimentin (hVIM) (1:200, SP20, Abcam, Cambridge, UK) [25,27,33,34]. Corre-

sponding isotype controls—normal mouse IgG_{2a} (X0943, Agilent Technologies), normal goat IgG (NI02, MilliporeSigma), and normal rabbit IgG (X0903, Agilent)—were applied at the same concentrations as their respective primary antibodies.

For detection, horseradish peroxidase (HRP)-conjugated secondary antibodies were used: goat anti-mouse (1:1000, 115-035-166, Jackson ImmunoResearch, West Grove, PA, USA) for type II collagen, donkey anti-goat (1:1000, 705-035-147, Jackson ImmunoResearch) for type I collagen and aggrecan, and goat anti-rabbit (1:1000, 111-035-144, Jackson ImmunoResearch) for human vimentin. Visualization was achieved using ImmPACT DAB Peroxidase (HRP) Substrate (SK-4105, Vector Laboratories, Burlingame, CA, USA). Brightfield images were captured using a BX41 microscope (Olympus, Tokyo, Japan) and processed with AmScope software. Detailed listings of all primary and secondary antibodies are available in **Supplementary Tables 1 and 2** [25,27,33,34].

RNA-Seq and Analysis

RNA was extracted from harvested cell sheets using RNeasy mini kit (74104, Qiagen, Hilden, Germany). After RNA integrity and quantity was checked, a complementary DNA (cDNA) library was constructed and used for pair-end sequencing using NovaSeq 6000 (Illumina, San Diego, CA, USA). Sequencing data were uploaded to the Galaxy web platform, and a public server at https://usegalaxy.org was used to analyze the data [35]. After trimming of Illumina-specific sequences using Trimmomatic version 0.38 [36], the sequence reads were aligned to the human genome reference sequence (hg38) using STAR version 2.7.5b [37]. Gene-level assignment was performed using featureCounts version 1.6.4 [38]. Acquired data quality was checked using MultiQC [39] and confirmed to be high. The gene expression matrix with raw gene counts was used for differential gene expression analysis using DESeq2 version 1.22.1 [40]. Clustering analysis was performed with differentially expressed 1554 genes of Padj <0.05, fold change $>$ Abs(2). Gene ontology (GO) analysis was performed using the Metascape platform at https://metascape.org [41] with the differentially expressed gene list of Padj <0.05, fold change >2 or fold change <-2. Gene set enrichment analysis (GSEA) was performed by GSEA platform (version 4.3.2, Broad institute (https://www.gsea-msigdb.org)) [42] on normalized counts of each sequenced sample. Pathway analysis was performed using ingenuity pathway analysis (IPA) (Qiagen) [43].

Interferon-γ Supplementation Culture

Based on our previous study using mesenchymal stromal cells [44,45], a 0, 2.5, or 25 ng/mL recombinant interferon gamma (IFN-γ) (I17001, Sigma-Aldrich) was added to P2 passage culture (2000 cells/cm^2) or cell sheet culture (10,000 cells/cm^2) for the entire 6 days or 14 days, respectively. Media were refreshed every 2–4 days. Subsequent chondrogenic pellet cultures were performed using single cells isolated from passage culture at day 6 or cell sheets at day 14.

Chondrogenic Differentiation Culture

Chondrogenic pellet culture was conducted following established protocols from previous studies [25,46]. JCCs and ACCs cultured until the end of passage 2, as well as collagenase-isolated cells from JCC sheets, were suspended in chondrocyte culture medium containing ascorbic acid. A total of 2.5×10^5 cells were placed into 15 mL conical tubes for pellet formation. The tubes were centrifuged at 500 $\times$g for 10 minutes, and the cells were incubated at 37 °C with 5 % CO_2 for 3 days to promote pellet development. After this initial incubation, the samples were treated with chondrogenic medium and transferred to a hypoxic incubator (37 °C, 5 % CO_2, 5 % O_2).

The chondrogenic medium used for pellet cultures consisted of high glucose-DMEM supplemented with the following components: 10 ng/mL transforming growth factor beta-3 (TGF-β3, 100-36E, Peprotech, Cranbury, NJ, USA), 20 ng/mL bone morphogenic protein-6 (120-06, BMP-6, PeproTech), 1 % Insulin-Transferrin-Selenium (41400045, ITS-G, ThermoFisher), 1 % penicillin-streptomycin (PS, 15140122, ThermoFisher), 1 % non-essential amino acids (11140050, NEAA, ThermoFisher), 100 nM dexamethasone (02194561-CF, MP Biomedicals, Irvine, CA, USA), 1.25 mg/mL bovine serum albumin (A2058, BSA, MilliporeSigma), 50 μg/mL L-ascorbic acid phosphate magnesium salt n-hydrate (Fujifilm Wako, 013-12061, Osaka, Japan), 40 μg/mL L-proline (P5607, MilliporeSigma), and 5.35 μg/mL linoleic acid (L1012, MilliporeSigma). The culture medium was refreshed twice per week over a period of 3 weeks [25,46].

Sulfated Glycosaminoglycan Quantification

Sulfated glycosaminoglycan (sGAG) content of differentiation culture samples was quantified using a well-established 1,9-dimethyl methylene blue (DMB) assay [47] utilizing chondroitin sulfate (PHR1786, MilliporeSigma) as a measurement standard. Each sample was mechanically pulverized with a Teflon pestle in a microcentrifuge tube, then digested for 24–48 hours in a buffered solution of papain from *C. papaya* (76216, MilliporeSigma). In a low-light environment, 135 μL of DMB dye (341088, MilliporeSigma) was distributed into each well of a 96-well plate along with a total volume of 40 μL of sample and papain solution adjusted to be within range of the chondroitin sulfate standards which were added in increments of 5 μg/μL from 0 to 35 μg/μL. The samples were scanned with a spectrometer (Cytation 3 image reader, BioTek, Winooski, VT, USA) at 595 nm.

Results

Juvenile Cartilage-Derived Chondrocytes Exhibit More Rapid Cell Growth, Higher Colony Forming Efficiency, and High Yield Compared to Adult Cartilage-Derived Chondrocytes

Current cartilage therapies (e.g., autologous chondrocyte implantation, ACI) face major scalability hurdles. Polydactyly-sourced juvenile cartilage-derived chondrocytes (JCCs) were therefore compared to femoral head adult FAI cartilage-derived chondrocytes (ACCs). Isolated cell number per milligram of cartilage tissue significantly declined with age, but no clear tendency is evident under 4 years of age (Fig. 1**A**). Both cell types show substrate adherence in primary cell culture, but ACC initiation of cell division is slow, while JCCs demonstrate markedly rapid, immediate proliferation (Fig. 1**B**). Colony forming efficiency in primary culture was significantly higher in JCCs compared to ACCs, suggesting higher growth potential and scalability for JCCs compared to ACCs (Fig. 1**C**). Interestingly, colony sizes and morphologies were heterogenous in both groups (Fig. 1**C**), but these colony differences disappeared after passaging the cells (data not shown), suggesting that dramatic clonal selections occur at early passages. Morphological differences of both cultured cell types became more evident as early as passage 2: The majority of ACCs exhibit larger, elongated shapes consistent with dedifferentiating chondrocytes compared to JCCs (Fig. 1**D**). Both cell types exhibited sustained growth and expansion potential (discontinued after 13 passages) with JCCs demonstrating more consistent and rapid population doubling rates through long-term passaging cultures (Fig. 1**E**).

In Vitro Evaluation of Juvenile Cartilage Derived Chondrocyte Sheets

Both JCCs and ACCs cultured on temperature-responsive cell culture inserts reached confluence by day 10 and maintained confluency for >4 days (Fig. 2**A**). This enabled consistent cell sheet harvest at day 14 of these cultures (Fig. 2**B**). Viabilities of cells in both chondrocyte sheets were very high (JCC sheets: 97.9 ± 1.3 %; ACC sheets: 97.2 ± 1.6 %). Freshly harvested, neither cell sheet stains with Safranin-O, an indicator of sulfated glycosaminoglycans (Fig. 2**C**). Interestingly, harvested JCC sheet thickness was twice that of ACC sheets (Fig. 2**C,D**) and total cell number per ACC sheet was almost half compared to JCC sheet (JCC sheet: $1.96 \pm 0.55 \times 10^6$ cells; ACC sheet: $0.97 \pm 0.17 \times 10^6$ cells), suggesting that cell densities in JCC and ACC sheets are comparable (Fig. 2**D**). Based on these yields, the theoretical numbers of JCC/ACC sheets able to be prepared from a single donor at a given passage are shown in Fig. 2**E** by dividing the total cell yield from each passage by the cell number of 42,000 required for a single cell sheet preparation. Notably, sheet yield numbers are 20 times higher in JCC sheets than ACC sheets at passage 2, which has been used in a recent clinical study, and these differences increase through extended passaged culture. Cell surface markers for ACC sheet purity and phenotype show profiles with few impurities (**Supplementary Fig. 1**), indicating that isolation and sheet culture processes are free of problematic contaminants and retain essential chondrocyte-specific traits.

In Vivo Evaluation of Regenerative Efficacy Using a Rodent Defect Model

To assess the regenerative potential of cell sheets *in vivo*, JCC and ACC sheets were implanted during the surgical induction of focal chondral defects in athymic rats. Four experimental groups were established: single-layer ACC sheet, bilayer ACC sheets, single-layer JCC sheet, and a defect-only negative control group. After 4 weeks, the defect sites were examined using stereomicroscopy, followed by histological analysis post-necropsy for comparative evaluation. In the defect-only group, a depressed tissue surface and fibrotic pannus were observed, indicating unsuccessful spontaneous cartilage regeneration (Fig. 3**A**). In contrast, all treatment groups showed neocartilage formation at the defect sites within 4 weeks (Fig. 3**A**). Safranin-O staining revealed that the defect-only group lacked staining, while all treated groups exhibited thick, Safranin-O-positive hyaline neocartilage (Fig. 3**A**). Notably, the interface between the regenerated cartilage and adjacent native lateral cartilage was well-integrated in all transplantation groups (Fig. 3**A**). Modified O'Driscoll scores based on Safranin-O-stained histological samples indicated substantial cartilage regeneration in all treatment groups compared to the defect-only group (Fig. 3**B**). Interestingly, the regenerated cartilage in the single JCC sheet group was approximately twice as thick as that in the single ACC sheet group (Fig. 3**C**). No signs of tumorigenesis or abnormal tissue formation were observed in any of the rats receiving cell sheet transplants, supporting the safety of the procedure.

Immunohistochemical analysis was performed on harvested knee samples to evaluate the expression of cartilage-specific matrix proteins aggrecan (ACAN) and type II collagen (COL2), as well as type I collagen (COL1), a marker of cartilage damage. In the defect-only group, pannus tissue lacked ACAN and COL2 expression but showed widespread COL1 expression (Fig. 3**A**). In contrast, neocartilage from all treatment groups exhibited COL1 expression at the surface and elevated ACAN and COL2 expression within the neocartilage matrix (Fig. 3**A**). Human-specific vimentin was detected in neocartilage regions of all transplantation groups, but not in the defect-only group, confirming that the regenerated tissue originated from the transplanted human cell sheets (Fig. 3**A**).

Molecular Characteristics of JCC Sheets and ACC Sheets

To compare the transcriptome profiles of JCC versus ACC sheets, RNAseq data from 13 JCC and 8 ACC

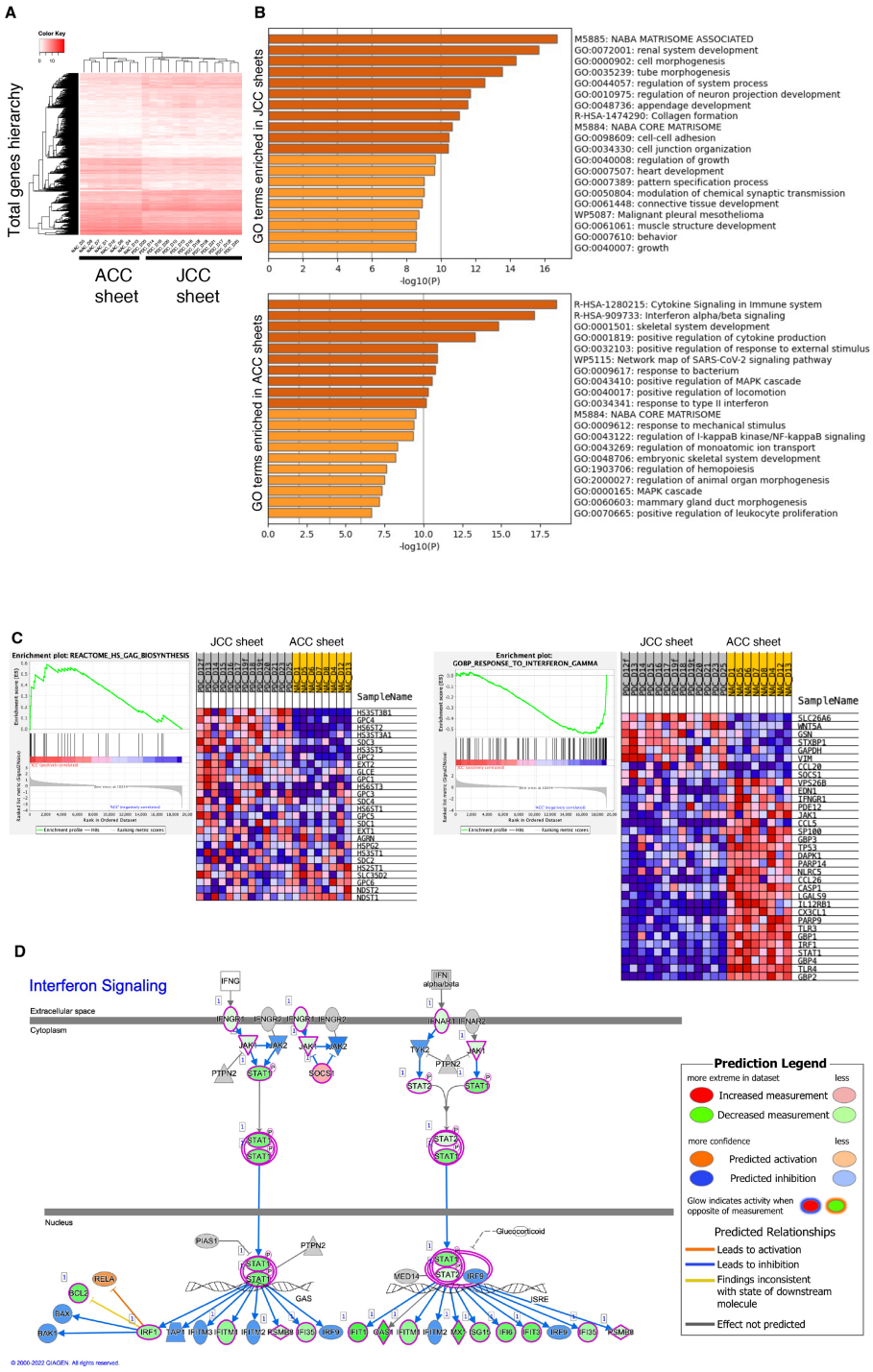

Fig. 4. Transcriptome analysis of chondrocyte sheets. (**A**) Hierarchical analysis of all JCC and ACC chondrocyte sheet samples; n = 8 ACC sheets; n = 13 JCC sheets. (**B**) Tables of GO analysis results showing the top 20 terms with the highest statistical significance. Top: GO terms enriched in JCC sheets, Bottom: GO terms enriched in ACC sheets. (**C**) Representative gene sets enriched in each sheet group. Left shows heparan sulfate glycosaminoglycan (HS-GAG) biosynthesis gene set and right shows the gene set for IFN-γ response. (**D**) Interferon signaling pathway identified as the most significantly different pathway between JCC and ACC. Significantly different pathway list can be found in **Supplementary Fig. 4**. Images were created with (**A**) Galaxy, (**B**) Metascape, (**C**) GSEA, and (**D**) ingenuity pathway analysis. GO, gene ontology; IFN-γ, interferon gamma; GSEA, gene set enrichment analysis.

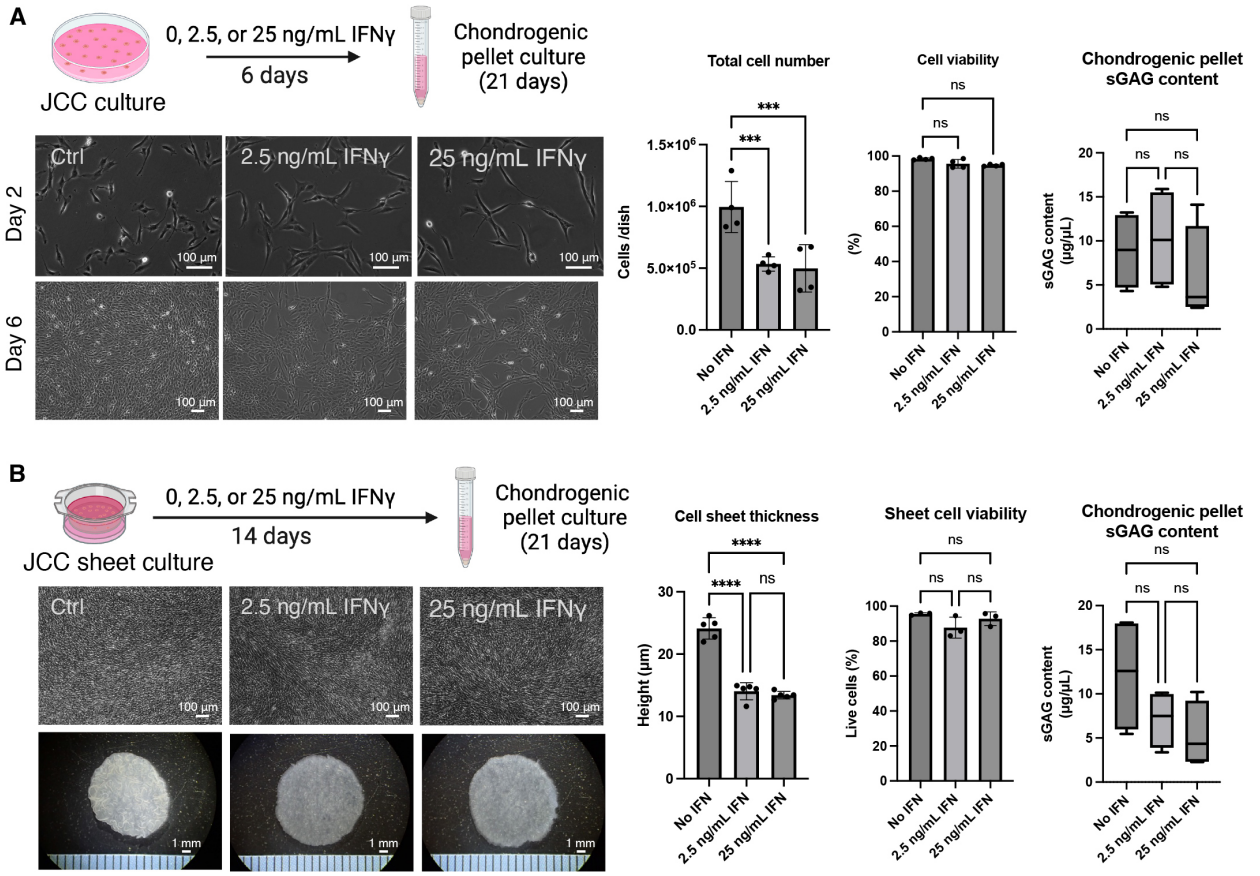

Fig. 5. IFN-γ effects on both chondrocyte passaging and cell sheet culture. (**A**) IFN-γ effects on JCC passage cultures. Left: photos of P2 JCC, with or without adding 2.5 ng/mL IFN-γ, or 25 ng/mL IFN-γ, at day 2 and day 6. Scale bars: 100 μm (both top and bottom). Right: total cell number and cell viability at day 6. Rightmost: sGAG content after 21-day chondrogenic pellet culture of the IFN-γ-treated cells. ***$p < 0.001$; ns, non-significant. (**B**) Left: confluent cell morphology at 2 weeks of culture (scale bars of top images: 100 μm) and cell sheet macroscopic images (scale intervals: 1 mm). Right: IFN-γ effects on cell sheet thickness and cell viability of harvested cell sheets at day 14. Rightmost: chondrogenic pellet sGAG content from cells isolated from IFN-γ-treated cell sheets. ****$p < 0.0001$; ns, non-significant with ANOVA and Tukey test. sGAG, sulfated glycosaminoglycan. Graphs were prepared using GraphPad Prism.

sheets from individual donors were analyzed, and differential gene expression data were obtained. Unsupervised hierarchical analysis shows two distinct data groupings between ACC and JCC sheets (Fig. 4**A**). Gene ontology (GO) analysis profiles GOs related to matrix production and cartilage development were highly enriched in JCC sheets, whereas ACC sheets showed multiple inflammation-related GOs (Fig. 4**B**, **Supplementary Table 3**). The most differentially expressed genes are shown in **Supplementary Fig. 2**. Among several gene set enrichment analysis (GSEA) results, the heparan sulfate and glycosaminoglycan biosynthesis gene set was significantly enriched in the JCC sheet group, whereas multiple interferon (IFN)-related gene sets were significantly enriched in the ACC sheet group (Fig. 4**C**, **Supplementary Fig. 3**). Furthermore, ingenuity pathway analysis (IPA) evidenced highest enrichment in IFN-γ signaling between JCC and ACC sheet samples (Fig. 4**D**, **Supplementary Fig. 4**). Taken together, interferon signaling activation appears as the most significant molecular signature distinguishing ACC from JCC sheets.

IFN-γ Signaling Hampers Chondrocyte Proliferative Potential

To further examine the role of IFN signaling in scalability of chondrocyte-based cell expansion for possible product manufacturing, JCC *in vitro* cell growth and chondrogenic capacity were analyzed. Since RNAseq showed no detection or very low sequence reads of IFN genes (*IFNAs*, *IFNB1*, *IFNG*, *IFNK*, and *IFNW1*, data not shown, but available at Gene Expression Omnibus (https://www.

ncbi.nlm.nih.gov/geo/)), involvement of endogenous IFNs was considered negligible. Therefore, we tested exogenous IFN effects on JCCs, rather than performing IFN-γ inhibitory experiments on ACCs. JCCs cultured in IFN-γ-supplemented media exhibit more elongated cell morphology compared to control conditions (Fig. 5**A**). JCC cultures with 2.5 ng/mL and 25 ng/mL IFN-γ similarly decrease their cell growth rates. Interestingly, JCC growth rates with IFN-γ are significantly slower than control cultures without observable effects on cell viability at one week of culture (Fig. 5**A**). Moreover, JCC cell sheet thickness at harvest was significantly reduced with viability unchanged by IFN-γ exposure (Fig. 5**B**). Sulfated glycosaminoglycan content in JCC chondrogenic pellet cultures was not significantly affected by extrinsic IFN-γ, both in passage and cell sheet culture exposure prior to further chondrogenic pellet culture (Fig. 5**A,B**). JCC pellet DNA did not show any significant differences from IFN supplementation, likely because pellet culture conditions were dedicated to chondrogenic differentiation with minimal proliferation phase (**Supplementary Fig. 5**).

Discussion

Due to high grafting costs, variable efficacy and tissue availability, current clinical demands for treating cartilage defects and osteoarthritis remain unsatisfied despite available approaches [48,49]. Cartistem is currently the only commercially available allogeneic and scalable product based on mesenchymal stem/stromal cells (MSCs), and it is approved for clinical use exclusively in Republic of Korea [50]. Our study assessed properties and the scalability of juvenile and adult cartilage tissue-derived scaffold-free cell sheets for cartilage repair and regeneration.

Juvenile cartilage cell sourcing gives rise to approximately 10 times more isolated cells compared to adult cartilage tissue (Fig. 1**A**), significantly impacting prospective scalability. In addition, colony forming efficiency was notably high (see Fig. 2**C**) compared to previously reported various mesenchymal stem/stromal cells (MSCs) isolated from bone marrow, adipose, or skin tissues [28,51–53]. This may be due to intrinsic heterogeneity of MSCs cultured from these tissues [54]. Cells cultured in chondrocyte culture medium from cartilage surgical discards may be relatively homogenous in high numbers of colony-forming cells. In fact, high cell purity was confirmed both in adult (**Supplementary Fig. 1**) and juvenile cartilage-derived chondrocytes [24,25]. Such homogeneity is beneficial for tissue engineering quality control, but careful monitoring of cell property and phenotypic changes during passaging is required for scaled production. Also, this study employed commonly available cartilage tissue harvests from different anatomical areas. Chondrocyte characteristics unique to different anatomical sources should be better stratified in future studies using more patient samples in addition to previous reports about other anatomical cell sources [55,56].

Our previous study using adult cartilage-derived chondrocytes harvested from femoral heads revealed approximately 50 % of cells remain viable at tissue harvest and cell isolation, but cultured cells exhibited high viability and cell growth potential, likely due to clonal selection by sub-culture [27]. This evidence suggests allogeneic utility for adult chondrocyte sources. Other groups have also reported that juvenile cartilage-derived chondrocytes from polydactyly digits [11] and deceased patients' knee cartilage [12] show higher proliferative capacity. Interestingly, particulated juvenile cartilage tissue contains higher ratios of proliferating cells compared to adult cartilage tissues sources [57]. The current study using multiple JCC and ACC donor samples demonstrates high viabilities of cell sheets cultured from both sources, but JCCs exhibit higher *in vitro* proliferation capacity (Fig. 1**B–E**). Given the high number of sheets theoretically possible from passaging (Fig. 2**E**), these cell types, especially JCCs, are attractive for future off-the-shelf commercial scaling opportunities.

A prior study showed that cartilage formation potential from juvenile and adult cartilage-derived chondrocytes is comparable in three-dimensional biomimetic hydrogels, with chondrogenic genes upregulated in juvenile cartilage-derived chondrocytes [58]. Other groups reported higher *in vitro* differentiation potential in juvenile cartilage-derived chondrocytes (i.e., glycosaminoglycan amounts and tissue compression modulus) [11,12]. Moreover, in poly-L-lactic acid (PLLA) scaffolds, rapidly proliferating cells can create larger toluidine blue-stained tissue when encapsulated and implanted *in vivo* [59]. In a previous study, adult cartilage-derived cell sheets are prepared from total knee arthroplasty (TKA) patient samples [24]. The TKA-derived chondrocyte sheets are prepared by coculture with synovial cells that support chondrocyte growth. In addition, the TKA sheets are triple-layered before transplantation, intending to enhance cartilage regeneration. Our adolescent FAI patients' femoral head-derived chondrocyte sheets showed structurely mature hyaline cartilage in the rat transplantation model both from single and double-layered translants, indicating high growth and regenerative potential in adolescent cartilage sources. Using modified O'Driscoll scoring system on histology samples and cell-source efficacy stratification [60], we have for the first time demonstrated the connection between specific *in vitro* properties and thick neocartilage formation capacity *in vivo* by implanting highly proliferative JCC sheets compared to ACC sheets without supporting biomaterials scaffolds and their associated confounding effects on chondrocyte expansion. These observations, taken together, suggest that cartilage formation *in vivo* requires high proliferative traits of the implanted cells with prerequisite chondrogenic potentials; JCCs fill this need. Biomechanical features of resulting neocartilage will be assessed in future studies.

Global gene expression comparisons between adult and juvenile sources distinguished multiple GOs and path-

ways including heparan sulfate glycosaminoglycan (HS-GAG) and inflammatory signatures from ACC sheets (Fig. 4**A–D**). HS-GAG is responsible for controlling the interstitial fluid pressure of articular cartilage and hence its compressive stiffness and load-bearing properties. The elevated HS-GAG signaling may have promoted deposition of the extracellular matrix in the *in vivo* single JCC sheet transplantation (Fig. 3**A–C**). Chondrocyte expression of major IFNs in any RNAseq data from ACC and JCC sheets was not detectable. In addition, STAT1, which is downstream of IFN-γ, is known to be activated by other cytokine ligands (e.g., epidermal growth factor (EGF), platelet-derived growth factor (PDGF), Interleukin-6 (IL-6), IL-27) [61]. We found no differential expression of these genes in cell sheet samples, suggesting that ACC sheet IFN-γ signaling is persistently activated from FAI-sourced hip tissue rather than the chondrocyte culture procedure employed. IFN-γ has been utilized for MSC priming for tissue regeneration like fibrosis [44,54]. Exogenous IFN-γ hampered the proliferation of JCCs (Fig. 5**A**) and limited maximal construct thickness (Fig. 5**B**). Therefore, maintaining low IFN-γ signaling can serve as a marker for production scalability in chondrocyte-based products. Our data in chondrocytes indicate the importance of context-dependent use of IFN-γ considered for specific disease targets.

As ACC cartilage samples were obtained from patients with FAI, these cells may be affected by normal FAI-involved local tissue site inflammation. In fact, some inflammatory signatures are reported in FAI patient bone tissue samples [62]. Aging has also been associated with chronic low-grade inflammation [63]. Therefore, future studies using patient tissue sources should consider both endogenous inflammatory activation and donor age prior to tissue harvest for subsequent cell-based product manufacturing. Different IFN-γ concentrations in adult versus juvenile joint fluids may be important to query for further mechanistic understanding and as possible surrogate markers for donor cell quality in cartilage regeneration.

This study demonstrates the potential for commercial scalability of cell sheet therapies using JCC sheets and ACC sheets, with greater promise observed in JCCs. A previous study using the same immunodeficient rat xenotransplantation model reported no evidence of heterotopic ossification or immune rejection over six months [25]. While implementation of appropriate facility development, clinical study design, and quality control protocols is essential for the successful dissemination of this therapy, large-scale production is expected to significantly reduce manufacturing costs. This is attributable not only to the long-term cryopreservability of JCCs, which can be stored in liquid nitrogen for several years without compromising viability, but also to their high proliferative capacity combined with redifferentiation potential. A clinical study investigating allogeneic JCC transplantation for knee cartilage repair in humans reported functional improvement and safety at one-year follow-up [26], and patients have remained under catamnestic observation for over four years without major adverse events (unpublished data). These findings support the feasibility of scalable allogeneic cell sheet therapies as a promising strategy for regenerative medicine. However, potential risks remain, including the possibility of immune sensitization in allogeneic settings, variability in donor cell quality, and undesired tissue remodeling. Continued long-term monitoring and rigorous regulatory oversight will be critical to ensure safety and efficacy as clinical application expands.

Limitations of the study: In the animal sheet transplantation studies, we established that control and three sheet transplant groups (i.e., one JCC sheet, one ACC sheet, and two ACC sheets) would have similar total implanted cell numbers based on cell counting of each cell sheet. While the total cell number in each ACC sheets is approximately half of the JCC sheet, the cell dose in the animal transplant study cannot be controlled to be exactly the same. In addition, the role of activated IFN-γ signaling in ACCs with low functionality should be further validated by targeting downstream molecules within ACCs or by comparison with chondrocytes derived from healthy adult cartilage tissue.

Conclusions

Human JCCs exhibit distinct differences in both expansion cultures and cell sheet properties compared to ACCs. Significantly, these differences are shown to correlate with their respective *in vivo* cartilage regenerative responses in an athymic rat cartilage defect healing model. Bulk RNAseq comparison reveals significantly differentially expressed genes which reflect a gene ontology of increased extracellular matrix synthesis and decreased IFN pathway activation. Distinctions shown between JCC and ACC cells and their sheet products represent important regenerative screening value for JCCs in assessing utility for cartilage regeneration translational use. Additionally, the highly scalable JCC sheet strategy using banked polydactyly cells produces attractive commercialization advantages over ACC sources and their sheets, based on JCC proliferative characteristics and cartilage regenerative properties for cell sheet-based cartilage regenerative applications. Reliable cell source selection, chondrogenic capacity retention during expansion and banking, and sheet fabrication are essential for consistent, economical large-scale clinical translation to address unmet cartilage repair clinical needs.

List of Abbreviations

ACCs, adult cartilage-derived chondrocytes; ACI, autologous chondrocyte implantation; BMP-6, bone morphogenic protein-6; FAI, femoroacetabular impingement; GO, gene ontology; GSEA, gene set enrichment analysis; IFN, interferon; IPA, ingenuity pathway analysis; JCCs, juvenile cartilage-derived chondrocytes; TGF-β3, transforming growth factor beta-3; IFN-γ, interferon gamma; FBS,

fetal bovine serum; STR, short tandem repeat; ACAN, aggrecan; COL2, type II collagen; COL1, type I collagen; VIM, vimentin; ns, non-significant; MSCs, mesenchymal stem/stromal cells; TKA, total knee arthroplasty; HS-GAG, heparan sulfate glycosaminoglycan; HRP, horseradish peroxidase; sGAG, sulfated glycosaminoglycan; DMB, 1,9-dimethyl methylene blue; hVIM, human vimentin; IL-6, Interleukin-6.

Availability of Data and Materials

Data sets generated and/or analyzed during the current study are available from the corresponding author upon reasonable request. RNA-seq raw data were deposited in the Gene Expression Omnibus (https://www.ncbi.nlm.nih.gov/geo/) under accession no. GSE235008.

Author Contributions

MK and TO contributed to the design of this work. MK designed, performed, interpreted all experiments and analysis, and wrote the manuscript. KM performed animal experiments and interpreted the data. AJF acquired part of *in vitro* experiments and wrote and edited the manuscript. NFM interpret data and edited the manuscript. TGM provided adult cartilage samples and input for designing animal knee defect model. DTH and AAW harvested juvenile cartilage tissue. MS provided scientific inputs and edited the manuscript. DWG revised critically for important intellectual content. TO supervised the technical teams, coordinated resources, and reviewed the manuscript. All authors read and approved the final manuscript. All authors agree to be accountable for all aspects of the work in ensuring that questions related to the accuracy or integrity of any part of the work are appropriately investigated and resolved.

Ethics Approval and Consent to Participate

The study was reviewed by the University of Utah Institutional Review Board (IRB): Both juvenile and adult surgical discard materials were deemed to be IRB-exempt due to use of the de-identified routine surgical discards. No ethical permission number was assigned and no informed consent was required. The animal study protocol was reviewed and approved by the Institutional Animal Care and Use Committee (IACUC) at the University of Utah (Protocol ID: 17-09011).

Acknowledgments

We thank Drs. S. Kameishi, K. Kim, C. Dunn, H. Thorp, S. Bou-Ghannam, and C.J. Reid for their comments and technical assistance on this study. The University of Utah HSC Core Flow Cytometry Facility and Huntsman Cancer Institute and The University of Utah High-throughput Genomics and Bioinformatic Analysis Core Facility are acknowledged as a valued technical resource.

Funding

This work was supported in part by the University Technology Acceleration Grant (UTAG) from the Utah Science, Technology, and Research (USTAR) program to DWG and TO, The University of Utah Research Incentive Seed Grant to MK, and American Orthopaedic Society for Sports Medicine AOSSM-JRF Allograft Research Grant to MK (#989015).

Conflict of Interest

TO is a shareholder of CellSeed, Inc. and is an inventor/developer designated on the patent for thermo-responsive cultureware. TGM is a paid speaker and consultant of Arthrex Inc. All other authors declare that they have no competing interests.

Supplementary Material

Supplementary material associated with this article can be found, in the online version, at https://doi.org/10.22203/eCM.v054a01.

References

[1] Huey DJ, Hu JC, Athanasiou KA. Unlike bone, cartilage regeneration remains elusive. Science. 2012; 338: 917–921. https://doi.org/10.1126/science.1222454.

[2] Flanigan DC, Harris JD, Trinh TQ, Siston RA, Brophy RH. Prevalence of chondral defects in athletes' knees: a systematic review. Medicine and Science in Sports and Exercise. 2010; 42: 1795–1801. https://doi.org/10.1249/MSS.0b013e3181d9eea0.

[3] Houck DA, Kraeutler MJ, Belk JW, Frank RM, McCarty EC, Bravman JT. Do Focal Chondral Defects of the Knee Increase the Risk for Progression to Osteoarthritis? A Review of the Literature. Orthopaedic Journal of Sports Medicine. 2018; 6: 2325967118801931. https://doi.org/10.1177/2325967118801931.

[4] Nuelle CW, Nuelle JAV, Cook JL, Stannard JP. Patient Factors, Donor Age, and Graft Storage Duration Affect Osteochondral Allograft Outcomes in Knees with or without Comorbidities. The Journal of Knee Surgery. 2017; 30: 179–184. https://doi.org/10.1055/s-0036-1584183.

[5] Farr J, Tabet SK, Margerrison E, Cole BJ. Clinical, Radiographic, and Histological Outcomes After Cartilage Repair With Particulated Juvenile Articular Cartilage: A 2-Year Prospective Study. The American Journal of Sports Medicine. 2014; 42: 1417–1425. https://doi.org/10.1177/0363546514528671.

[6] Negoro T, Takagaki Y, Okura H, Matsuyama A. Trends in clinical trials for articular cartilage repair by cell therapy. NPJ Regenerative Medicine. 2018; 3: 17. https://doi.org/10.1038/s41536-018-0055-2.

[7] Thorp H, Kim K, Kondo M, Maak T, Grainger DW, Okano T. Trends in Articular Cartilage Tissue Engineering: 3D Mesenchymal Stem Cell Sheets as Candidates for Engineered Hyaline-Like Cartilage. Cells. 2021; 10: 643. https://doi.org/10.3390/cells10030643.

[8] Kwon H, Brown WE, Lee CA, Wang D, Paschos N, Hu JC, *et al.* Surgical and tissue engineering strategies for articular cartilage and meniscus repair. Nature Reviews. Rheumatology. 2019; 15: 550–570. https://doi.org/10.1038/s41584-019-0255-1.

[9] Deinsberger J, Reisinger D, Weber B. Global trends in clinical trials involving pluripotent stem cells: a systematic multi-database analysis. NPJ Regenerative Medicine. 2020; 5: 15. https://doi.org/10.1038/s41536-020-00100-4.

[10] Nasu M, Takayama S, Umezawa A. Efficiency of Human Epiphyseal Chondrocytes with Differential Replication Numbers for Cellu-

lar Therapy Products. BioMed Research International. 2016; 2016: 6437658. https://doi.org/10.1155/2016/6437658.

[11] Cavalli E, Levinson C, Hertl M, Broguiere N, Brück O, Mustjoki S, *et al*. Characterization of polydactyly chondrocytes and their use in cartilage engineering. Scientific Reports. 2019; 9: 4275. https://doi.org/10.1038/s41598-019-40575-w.

[12] Adkisson HD 4th, Martin JA, Amendola RL, Milliman C, Mauch KA, Katwal AB, *et al*. The potential of human allogeneic juvenile chondrocytes for restoration of articular cartilage. The American Journal of Sports Medicine. 2010; 38: 1324–1333. https://doi.org/10.1177/0363546510361950.

[13] Adkisson HD, Milliman C, Zhang X, Mauch K, Maziarz RT, Streeter PR. Immune evasion by neocartilage-derived chondrocytes: Implications for biologic repair of joint articular cartilage. Stem Cell Research. 2010; 4: 57–68. https://doi.org/10.1016/j.scr.2009.09.004.

[14] Kushida A, Yamato M, Konno C, Kikuchi A, Sakurai Y, Okano T. Decrease in culture temperature releases monolayer endothelial cell sheets together with deposited fibronectin matrix from temperature-responsive culture surfaces. Journal of Biomedical Materials Research. 1999; 45: 355–362. https://doi.org/10.1002/(sici)1097-4636(19990615)45:4<355::aid-jbm10>3.0.co;2-7.

[15] Kobayashi J, Kikuchi A, Aoyagi T, Okano T. Cell sheet tissue engineering: Cell sheet preparation, harvesting/manipulation, and transplantation. Journal of Biomedical Materials Research. Part A. 2019; 107: 955–967. https://doi.org/10.1002/jbm.a.36627.

[16] Okano T, Yamada N, Sakai H, Sakurai Y. A novel recovery system for cultured cells using plasma-treated polystyrene dishes grafted with poly(N-isopropylacrylamide). Journal of Biomedical Materials Research. 1993; 27: 1243–1251. https://doi.org/10.1002/jbm.820271005.

[17] Nishida K, Yamato M, Hayashida Y, Watanabe K, Yamamoto K, Adachi E, *et al*. Corneal reconstruction with tissue-engineered cell sheets composed of autologous oral mucosal epithelium. The New England Journal of Medicine. 2004; 351: 1187–1196. https://doi.org/10.1056/NEJMoa040455.

[18] Sawa Y, Miyagawa S, Sakaguchi T, Fujita T, Matsuyama A, Saito A, *et al*. Tissue engineered myoblast sheets improved cardiac function sufficiently to discontinue LVAS in a patient with DCM: report of a case. Surgery Today. 2012; 42: 181–184. https://doi.org/10.1007/s00595-011-0106-4.

[19] Yamamoto K, Yamato M, Morino T, Sugiyama H, Takagi R, Yaguchi Y, *et al*. Middle ear mucosal regeneration by tissue-engineered cell sheet transplantation. NPJ Regenerative Medicine. 2017; 2: 6. https://doi.org/10.1038/s41536-017-0010-7.

[20] Kanzaki M, Takagi R, Washio K, Kokubo M, Yamato M. Bioartificial pleura using an autologous dermal fibroblast sheet. NPJ Regenerative Medicine. 2017; 2: 26. https://doi.org/10.1038/s41536-017-0031-2.

[21] Iwata T, Yamato M, Washio K, Yoshida T, Tsumanuma Y, Yamada A, *et al*. Periodontal regeneration with autologous periodontal ligament-derived cell sheets-A safety and efficacy study in ten patients. Regenerative Therapy. 2018; 9: 38–44. https://doi.org/10.1016/j.reth.2018.07.002.

[22] Ohki T, Yamato M, Ota M, Takagi R, Murakami D, Kondo M, *et al*. Prevention of esophageal stricture after endoscopic submucosal dissection using tissue-engineered cell sheets. Gastroenterology. 2012; 143: 582–588.e2. https://doi.org/10.1053/j.gastro.2012.04.050.

[23] Sato M, Yamato M, Mitani G, Takagaki T, Hamahashi K, Nakamura Y, *et al*. Combined surgery and chondrocyte cell-sheet transplantation improves clinical and structural outcomes in knee osteoarthritis. NPJ Regenerative Medicine. 2019; 4: 4. https://doi.org/10.1038/s41536-019-0069-4.

[24] Maehara M, Sato M, Toyoda E, Takahashi T, Okada E, Kotoku T, *et al*. Characterization of polydactyly-derived chondrocyte sheets versus adult chondrocyte sheets for articular cartilage repair. Inflammation and Regeneration. 2017; 37: 22. https://doi.org/10.1186/s41232-017-0053-6.

[25] Kondo M, Kameishi S, Kim K, Metzler NF, Maak TG, Hutchinson DT, *et al*. Safety and efficacy of human juvenile chondrocyte-derived cell sheets for osteochondral defect treatment. NPJ Regenerative Medicine. 2021; 6: 65. https://doi.org/10.1038/s41536-021-00173-9.

[26] Hamahashi K, Toyoda E, Ishihara M, Mitani G, Takagaki T, Kaneshiro N, *et al*. Polydactyly-derived allogeneic chondrocyte cell-sheet transplantation with high tibial osteotomy as regenerative therapy for knee osteoarthritis. NPJ Regenerative Medicine. 2022; 7: 71. https://doi.org/10.1038/s41536-022-00272-1.

[27] Rogers MJ, Kondo M, Kim K, Okano T, Maak TG. Femoral Head Chondrocyte Viability at the Cam Deformity in Patients With Femoroacetabular Impingement Syndrome. The American Journal of Sports Medicine. 2020; 48: 3586–3593. https://doi.org/10.1177/0363546520962788.

[28] Cai H, Kondo M, Sandhow L, Xiao P, Johansson AS, Sasaki T, *et al*. Critical role of Lama4 for hematopoiesis regeneration and acute myeloid leukemia progression. Blood. 2022; 139: 3040–3057. https://doi.org/10.1182/blood.2021011510.

[29] Kondo M, Yamato M, Takagi R, Murakami D, Namiki H, Okano T. Significantly different proliferative potential of oral mucosal epithelial cells between six animal species. Journal of Biomedical Materials Research. Part A. 2014; 102: 1829–1837. https://doi.org/10.1002/jbm.a.34849.

[30] Qian H, Le Blanc K, Sigvardsson M. Primary mesenchymal stem and progenitor cells from bone marrow lack expression of CD44 protein. The Journal of Biological Chemistry. 2012; 287: 25795–25807. https://doi.org/10.1074/jbc.M112.339622.

[31] Rutgers M, van Pelt MJ, Dhert WJ, Creemers LB, Saris DB. Evaluation of histological scoring systems for tissue-engineered, repaired and osteoarthritic cartilage. Osteoarthritis and Cartilage/OARS, Osteoarthritis Research Society. 2010; 18: 12–23. https://doi.org/10.1016/j.joca.2009.08.009.

[32] Niederauer GG, Slivka MA, Leatherbury NC, Korvick DL, Harroff HH, Ehler WC, *et al*. Evaluation of multiphase implants for repair of focal osteochondral defects in goats. Biomaterials. 2000; 21: 2561–2574. https://doi.org/10.1016/S0142-9612(00)00124-1.

[33] Yamashita A, Morioka M, Yahara Y, Okada M, Kobayashi T, Kuriyama S, *et al*. Generation of scaffoldless hyaline cartilaginous tissue from human iPSCs. Stem Cell Reports. 2015; 4: 404–418. https://doi.org/10.1016/j.stemcr.2015.01.016.

[34] Itokazu M, Wakitani S, Mera H, Tamamura Y, Sato Y, Takagi M, *et al*. Transplantation of Scaffold-Free Cartilage-Like Cell-Sheets Made from Human Bone Marrow Mesenchymal Stem Cells for Cartilage Repair: A Preclinical Study. Cartilage. 2016; 7: 361–372. https://doi.org/10.1177/1947603515627342.

[35] Galaxy Community. The Galaxy platform for accessible, reproducible and collaborative biomedical analyses: 2022 update. Nucleic Acids Research. 2022; 50: W345–W351. https://doi.org/10.1093/nar/gkac247.

[36] Bolger AM, Lohse M, Usadel B. Trimmomatic: a flexible trimmer for Illumina sequence data. Bioinformatics. 2014; 30: 2114–2120. https://doi.org/10.1093/bioinformatics/btu170.

[37] Dobin A, Davis CA, Schlesinger F, Drenkow J, Zaleski C, Jha S, *et al*. STAR: ultrafast universal RNA-seq aligner. Bioinformatics. 2013; 29: 15–21. https://doi.org/10.1093/bioinformatics/bts635.

[38] Liao Y, Smyth GK, Shi W. featureCounts: an efficient general purpose program for assigning sequence reads to genomic features. Bioinformatics. 2014; 30: 923–930. https://doi.org/10.1093/bioinformatics/btt656.

[39] Ewels P, Magnusson M, Lundin S, Käller M. MultiQC: summarize analysis results for multiple tools and samples in a single report. Bioinformatics. 2016; 32: 3047–3048. https://doi.org/10.1093/bioinformatics/btw354.

[40] Love MI, Huber W, Anders S. Moderated estimation of fold change

and dispersion for RNA-seq data with DESeq2. Genome Biology. 2014; 15: 550. https://doi.org/10.1186/s13059-014-0550-8.

[41] Zhou Y, Zhou B, Pache L, Chang M, Khodabakhshi AH, Tanaseichuk O, *et al*. Metascape provides a biologist-oriented resource for the analysis of systems-level datasets. Nature Communications. 2019; 10: 1523. https://doi.org/10.1038/s41467-019-09234-6.

[42] Subramanian A, Tamayo P, Mootha VK, Mukherjee S, Ebert BL, Gillette MA, *et al*. Gene set enrichment analysis: a knowledge-based approach for interpreting genome-wide expression profiles. Proceedings of the National Academy of Sciences of the United States of America. 2005; 102: 15545–15550. https://doi.org/10.1073/pnas.0506580102.

[43] Krämer A, Green J, Pollard J Jr, Tugendreich S. Causal analysis approaches in Ingenuity Pathway Analysis. Bioinformatics. 2014; 30: 523–530. https://doi.org/10.1093/bioinformatics/btt703.

[44] Dunn CM, Kameishi S, Cho YK, Song SU, Grainger DW, Okano T. Interferon-Gamma Primed Human Clonal Mesenchymal Stromal Cell Sheets Exhibit Enhanced Immunosuppressive Function. Cells. 2022; 11: 3738. https://doi.org/10.3390/cells11233738.

[45] Philipp D, Suhr L, Wahlers T, Choi YH, Paunel-Görgülü A. Preconditioning of bone marrow-derived mesenchymal stem cells highly strengthens their potential to promote IL-6-dependent M2b polarization. Stem Cell Research & Therapy. 2018; 9: 286. https://doi.org/10.1186/s13287-018-1039-2.

[46] Thorp H, Kim K, Kondo M, Grainger DW, Okano T. Fabrication of hyaline-like cartilage constructs using mesenchymal stem cell sheets. Scientific Reports. 2020; 10: 20869. https://doi.org/10.1038/s41598-020-77842-0.

[47] Estes BT, Diekman BO, Gimble JM, Guilak F. Isolation of adipose-derived stem cells and their induction to a chondrogenic phenotype. Nature Protocols. 2010; 5: 1294–1311. https://doi.org/10.1038/nprot.2010.81.

[48] Cengiz IF, Pereira H, de Girolamo L, Cucchiarini M, Espregueira-Mendes J, Reis RL, *et al*. Orthopaedic regenerative tissue engineering en route to the holy grail: disequilibrium between the demand and the supply in the operating room. Journal of Experimental Orthopaedics. 2018; 5: 14. https://doi.org/10.1186/s40634-018-0133-9.

[49] Abou-El-Enein M, Elsanhoury A, Reinke P. Overcoming Challenges Facing Advanced Therapies in the EU Market. Cell Stem Cell. 2016; 19: 293–297. https://doi.org/10.1016/j.stem.2016.08.012.

[50] Jung SH, Nam BJ, Choi CH, Kim S, Jung M, Chung K, *et al*. Allogeneic umbilical cord blood-derived mesenchymal stem cell implantation versus microdrilling combined with high tibial osteotomy for cartilage regeneration. Scientific Reports. 2024; 14: 3333. https://doi.org/10.1038/s41598-024-53598-9.

[51] Dolinska M, Cai H, Månsson A, Shen J, Xiao P, Bouderlique T, *et al*. Characterization of the bone marrow niche in patients with chronic myeloid leukemia identifies CXCL14 as a new therapeutic option. Blood. 2023; 142: 73–89. https://doi.org/10.1182/blood.2022016896.

[52] Sandhow L, Cai H, Leonard E, Xiao P, Tomaipitinca L, Månsson A, *et al*. Skin mesenchymal niches maintain and protect AML-initiating stem cells. The Journal of Experimental Medicine. 2023; 220: e20220953. https://doi.org/10.1084/jem.20220953.

[53] Vishnubalaji R, Al-Nbaheen M, Kadalmani B, Aldahmash A, Ramesh T. Comparative investigation of the differentiation capability of bone-marrow- and adipose-derived mesenchymal stem cells by qualitative and quantitative analysis. Cell and Tissue Research. 2012; 347: 419–427. https://doi.org/10.1007/s00441-011-1306-3.

[54] Dunn CM, Kameishi S, Grainger DW, Okano T. Strategies to address mesenchymal stem/stromal cell heterogeneity in immunomodulatory profiles to improve cell-based therapies. Acta Biomaterialia. 2021: 133: 114–125. https://doi.org/10.1016/j.actbio.2021.03.069.

[55] Anderson DEJ, Athanasiou KA. A comparison of primary and passaged chondrocytes for use in engineering the temporomandibular joint. Archives of Oral Biology. 2009; 54: 138–145. https://doi.org/10.1016/j.archoralbio.2008.09.018.

[56] Kafienah W, Jakob M, Démarteau O, Frazer A, Barker MD, Martin I, *et al*. Three-dimensional tissue engineering of hyaline cartilage: comparison of adult nasal and articular chondrocytes. Tissue Engineering. 2002; 8: 817–826. https://doi.org/10.1089/10763270260424178.

[57] Zhang C, Zhao X, Ao Y, Cao J, Yang L, Duan X. Proliferation ability of particulated juvenile allograft cartilage. Journal of Orthopaedic Surgery and Research. 2021; 16: 56. https://doi.org/10.1186/s13018-020-02199-z.

[58] Smeriglio P, Lai JH, Dhulipala L, Behn AW, Goodman SB, Smith RL, *et al*. Comparative potential of juvenile and adult human articular chondrocytes for cartilage tissue formation in three-dimensional biomimetic hydrogels. Tissue Engineering. Part A. 2015; 21: 147–155. https://doi.org/10.1089/ten.tea.2014.0070.

[59] Ishibashi M, Hikita A, Fujihara Y, Takato T, Hoshi K. Human auricular chondrocytes with high proliferation rate show high production of cartilage matrix. Regenerative Therapy. 2017; 6: 21–28. https://doi.org/10.1016/j.reth.2016.11.001.

[60] Matsukura K, Kondo M, Metzler NF, Ford AJ, Maak TG, Hutchinson DT, *et al*. Regenerative Variability of Human Juvenile Chondrocyte Sheets From Different Cell Donors in an Athymic Rat Knee Chondral Defect Model. Cartilage. 2024; 19476035241277946. https://doi.org/10.1177/19476035241277946.

[61] Hu X, Li J, Fu M, Zhao X, Wang W. The JAK/STAT signaling pathway: from bench to clinic. Signal Transduction and Targeted Therapy. 2021; 6: 402. https://doi.org/10.1038/s41392-021-00791-1.

[62] Gao G, Wu R, Liu R, Wang J, Ao Y, Xu Y. Genes associated with inflammation and bone remodeling are highly expressed in the bone of patients with the early-stage cam-type femoroacetabular impingement. Journal of Orthopaedic Surgery and Research. 2021; 16: 348. https://doi.org/10.1186/s13018-021-02499-y.

[63] Sanchez-Lopez E, Coras R, Torres A, Lane NE, Guma M. Synovial inflammation in osteoarthritis progression. Nature Reviews. Rheumatology. 2022; 18: 258–275. https://doi.org/10.1038/s41584-022-00749-9.

Editor's note: The Scientific Editor responsible for this paper was Martin Stoddart.

Received: 31st October 2024; **Accepted**: 5th September 2025; **Published**: 28th November 2025